



Research paper

Cam synthesis applied to the design of a customized mandibular advancement device for the treatment of obstructive sleep apnea



A. Bataller^a, J.A. Cabrera^{a,*}, M. García^a, J.J. Castillo^a, P. Mayoral^b

^a Department of Mechanical Engineering, University of Málaga, C/ Doctor Ortiz Ramos s/n, Ampliación Campus Teatinos, Málaga 29071, Spain

^b Alfonso X el Sabio University, Madrid, Spain

ARTICLE INFO

Article history:

Received 22 January 2018

Accepted 7 February 2018

Available online 13 February 2018

Keywords:

Mandibular advancement device

Cam synthesis

Evolutionary algorithms

Mandible kinematics

ABSTRACT

Mandibular Advancement Devices (MAD) have proved to be effective in the treatment of slight to moderate Obstructive Sleep Apnea (OSA). These devices open the upper airways by keeping the jaw forward with respect to its resting position. To date, none of the available devices have taken into account the kinematic behavior of each patient's mandible. This work presents a customized MAD for the treatment of OSA. A study of the mandible kinematics is carried out to determine the relationship between mouth opening and mandible advancement. The device includes two cams, one on each side, to make the mandible move forward. The cam profile is designed using a Bezier cubic curve that is optimized by means of an evolutionary algorithm. The kinematics of each patient's mandible is taken into account to ensure that the jaw does not move backwards at any time while opening the mouth. A real case study is presented to validate the proposed methodology.

© 2018 Elsevier Ltd. All rights reserved.

1. Introduction

Sleep apnea is a common disorder in which a person stops breathing while sleeping [1,2]. It is a leading cause of excessive daytime sleepiness. The most common type of sleep apnea is Obstructive Sleep Apnea (OSA). Untreated sleep apnea increases the risk of developing cardiovascular diseases such as arrhythmias, heart failure and stroke [3–5].

OSA is a chronic disorder that requires long-term treatment [6]. Apart from lifestyle changes, the main treatment options are Continuous Positive Air Pressure (CPAP), Oral Appliances (OA) and surgery. A CPAP machine is a pump connected to a face or nose mask that forces air into the nasal passages at mild pressure to keep the upper airways continuously open. Oral appliances open the upper airway, either by mandibular repositioning or by keeping the tongue forward with respect to its resting position. The most used OA are Mandibular Advancement Devices (MAD). Their main advantages compared to CPAP are that they are soundless, economic, manageable and do not require power supply.

Sutherland et al. [7,8] compiled the results of different works that confirmed that most patients preferred using OA to CPAP treatment. Moreover, the effectiveness of OA has been validated in numerous studies [9–14].

There is a great variety of MAD models [7]. There are one-piece and two-piece devices. The first ones are manufactured for a predefined protrusion value while most two-piece devices can achieve different protrusion levels [15]. Both of them

* Corresponding author.

E-mail address: jcabrera@uma.es (J.A. Cabrera).

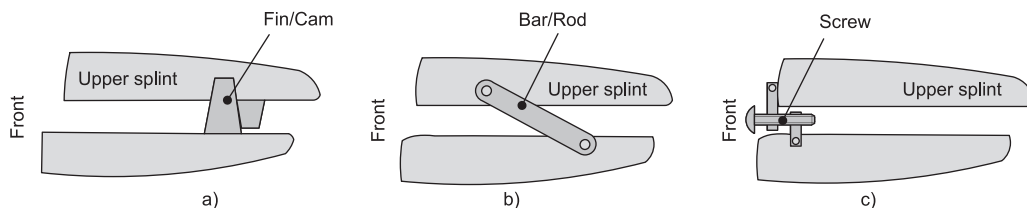


Fig. 1. Different systems used to couple the two plates of two-piece devices: (a) Fin or Cam (b) Bar or rod (c) Screw.

can be either prefabricated or custom-made. The splint of the latter is adapted to the patient's dentition in coordination with the dentist. It shows better results, mainly because of its improved overnight retention and protrusion control in contrast with the prefabricated devices [16].

There are different systems used to couple the two plates of two-piece devices, such as bars, elastic straps, springs, telescopic rods, tube connectors and lateral fins among others [17] (see Fig. 1). More than 70 oral appliances exist that have been approved by the FDA (U.S. Food & Drug Administration), each with their own advantages and disadvantages. The differences between the designs affect comfort and effectiveness. Customers prefer models with high freedom of mandibular movement (vertical and lateral) and maximum tongue space. Most patients do not feel comfortable with pieces occupying space in their mouth or metallic parts being in contact with their tongue. Devices with lateral fins (or cams) offer more comfort than other systems because they maximize tongue space, allow opening the mouth (to breathe, drink or talk) and permit mandibular lateral movement.

Comparative effectiveness studies for different MAD models have been accomplished by numerous researches [7,8,13,15,18–20]. These works have demonstrated that the effectiveness mainly depends on mandibular protrusion. Although the initial protrusion can be adjusted in all the studied models, protrusion varies in each model in a different way when patients open their mouth. Lawton et al. [18] affirmed that one of the patients' main complaints was that they woke up during the night and that their mandible had "slipped back". Although this problem was associated to a specific MAD model, it remarked the importance of the device design. The devices should not allow the jaw to move backwards at any time while opening the mouth. Other technical disadvantages of most two-piece adjustable devices are breakages and frequent adjustments [14,18]. These last problems are quite common in devices with bars, rods and connectors and less frequent in those designed with fins. This is mainly due to the fact that they do not have moving metallic parts.

To date, none of the existing devices have been manufactured considering each patient's mandibular kinematics, hence operating differently in each individual. Bloch et al. [15] stated in their work that the effect of a device might vary among different patients. Yow [21] assured that some factors needed to be studied to reach optimal long-term effectiveness. The device design and patients' characteristics stood out among these factors. According to Yow, it is essential to consider each patient's individual requirements. Teixeira et al. also pointed out differences in individual responses to OA therapy [22].

Focusing on devices with lateral fins or cams being used nowadays, none of them can guarantee that the mandible does not move backward when opening the mouth. This is due to the fact that they use straight lines for the profiles of the fin (in the mandible) and the follower (in the maxilla). Some of these MADs try to mitigate this limitation by adding lateral elastic hoods to close the mouth during the night.

MAD design can be improved by using cams with an optimized profile to assure that the jaw does not move backwards while opening the mouth. Numerous studies have presented different approaches for either kinematic or dynamic cam optimization [23–35]. Some of them have proposed the use of genetic algorithms [25,28,32] or evolutionary techniques [31]. Other methods are based on a unified optimization strategy, including a single objective optimization procedure for kinematics and a dynamic model for the cam-follower mechanism [34,35]. The cam design for a MAD does not need to take into account dynamic behavior. The cam profile can be optimized to guarantee that a point of the jaw follows a predefined path. Sahu et al. [36] reviewed the basic curves and splines used to design cam profiles by different researchers in the last twenty years. Bezier curves have frequently been used when dealing with non-complex curves that can be represented with a low number of precision points [24,30].

In this research the design of a customized two-piece MAD that contemplates patients' mandible kinematic behavior is presented. The protrusion control is assured by means of two cams, one at each side of the device. A deep study of mandible kinematics is carried out to establish the relationship between mouth opening and protrusion. In order to achieve the desired movement, the cam profile is optimized by means of an evolutionary algorithm developed by the authors of this work [37]. The final design guarantees that the mandible does not move backwards at any time while opening the mouth. The design also considers those factors that help to improve the comfort level such as high lateral movement, free tongue space, non-metallic pieces and a non-intrusive cam design.

This paper is structured as follows. In Section 2, a kinematic study of mandible movement is presented. Once the desired path for a point on the mandible has been specified, the optimal design of the cam is carried out in Section 3. Then, in Section 4, the developed method is applied to a real case. Section 5 analyses the results, which are used to create a virtual model in a 3D CAD-CAE parametric software application. This model is used to manufacture the device with a 3D printer. Finally, Section 6 draws the conclusions of this work.

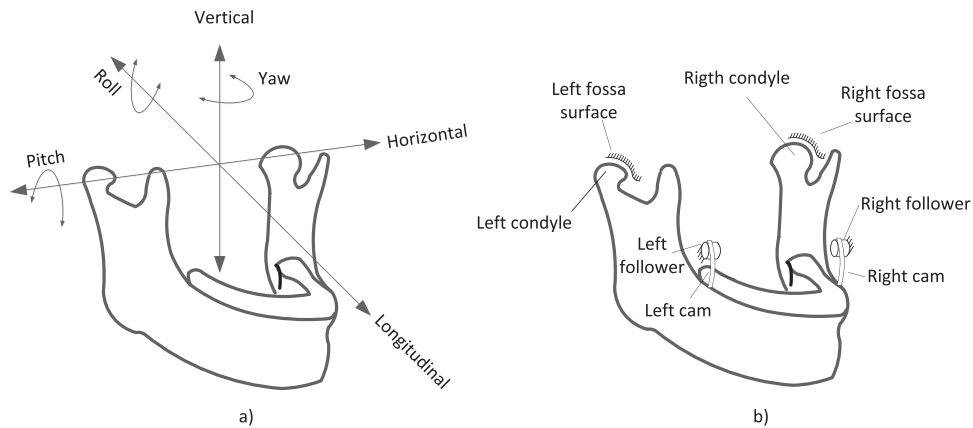


Fig. 2. (a) Mandible with six degrees of freedom. (b) Mandible with condyle and follower-cam constraints.

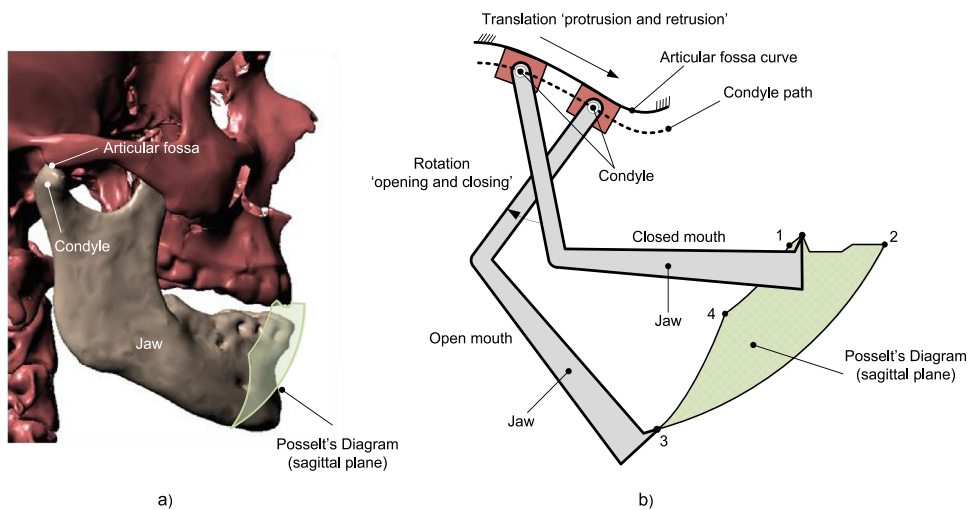


Fig. 3. (a) Real temporomandibular joint 3D model. (b) Kinematic scheme of the mechanism that reproduces jaw movement.

2. Kinematic model of mandibular movement

Mandible movement has six degrees of freedom. Rotation as well as translation can be carried out, about and along respectively, a horizontal, vertical and longitudinal axis (Fig. 2a). However, this movement is constrained by the temporomandibular joint. If the joint contact is considered to be rigid, the movement of the condyle in a direction perpendicular to the fossa surface is restricted (see Fig. 2b). This means that the condyle movements in the longitudinal and vertical directions are not independent from each other. Therefore, each joint eliminates one degree of freedom. Consequently, the functional movement of the jaw has four degrees of freedom [38]. By adding a follower and cam joint to each side of the mandible, two or three degrees of freedom are deducted depending whether the movement in the horizontal direction is allowed or not. Even in the case that the lateral movement is not restricted, its range is very low and the mandible is forced to move within the sagittal plane with one effective degree of freedom.

Fig. 3a shows a mandible 3D model obtained by means of a scanner. It displays how the temporomandibular joint between the mandible and the temporal bone is located in the articular fossa. The kinematic behavior of the jaw within the sagittal plane has been studied in multiple works [39–46]. Its movement is a composition of a rotation about an axis that goes through the two condyles and a translation along the articular fossa. When opening the mouth, the jaw moves forward while rotating.

Fig. 3b shows a kinematic scheme of a mechanism that reproduces mandibular movement in the sagittal plane. The temporomandibular joint is represented by means of a prismatic joint along a curve and a hinge. Therefore, the mechanism has two degrees of freedom (DOF).

The jaw is represented in two positions: the rest position with closed mouth and the maximum mouth opening position. In Fig. 3, Posselt's diagram shows the region in which the lower incisor can move [47]. Several borders that are fundamental for MAD customization can be identified in this region.

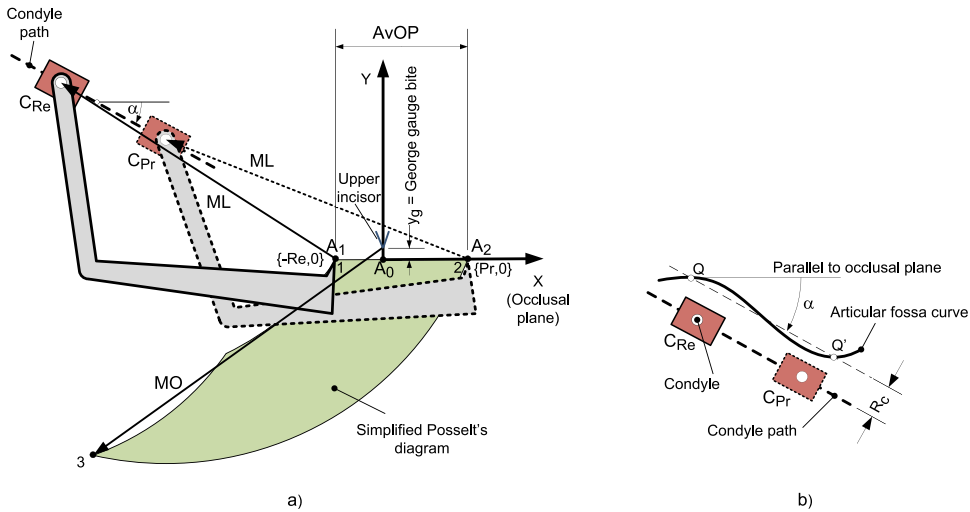


Fig. 4. (a) Mandible in its maximum retruded and protruded positions. (b) Definition of the condyle path by means of a straight line parallel to a line that goes through the maximum and minimum point of the articular fossa curve.

Point 1 represents the incisor position when the mandible is at its maximum retrusion. Segment 1–4 is an arc described by the incisor during the first part of the mouth opening movement. If the mouth continues opening after point 4, the mandible starts moving forward while rotating and the incisor describes path 4–3 reaching maximum protrusion and mouth opening. Next, if the mouth closes, maintaining the protrusion value, the incisor describes arc 3–2. Finally, the border from point 2 to point 1 is traced translating the jaw from maximum protrusion to maximum retrusion with slight up-and-down movements to avoid collision between the lower and upper incisor.

Fig. 4a shows a simplified representation of Posselt's diagram whose segments 1–2 and 2–3 are used for the cam design. A fixed reference system is defined, which is linked to the maxilla with the X axis parallel to the occlusal plane. The origin of the reference system is located in the lower incisor's initial position when protrusion and retrusion are measured with a George Gauge, a simple tool formed by a bite fork, a lower and upper notch and a millimeter indicator that enables dentists to make accurate measurements of the position of the jaw. In Fig. 4a, y_g is the distance from the lower and upper incisor that depends on the bite fork thickness. The standard values are 2 and 5 mm.

The jaw is displayed in maximum retrusion on the continuous line and in maximum protrusion on the dotted line. In this figure, segment 1–2 is represented by a straight line whose length, AvOP, is the sum of maximum protrusion (Pr) and retrusion (Re). Values Pr and Re can be measured in the sagittal plane by means of a George Gauge.

$$AvPO = \overline{1-2} = Re + Pr \tag{1}$$

In Fig. 4a, border 2–3 is the path described by the inferior incisor when opening the mouth with the jaw in the position of maximum protrusion. It can be drawn as an arc of a circle with radius ML and center C_{Pr}. Point 3 is the intersection between the previous arc and an arc with its center in the upper incisor and radius MO (maximum mouth opening). In order to know mandibular length, ML, a scanner or X-ray of the patient's mandible is required.

Actually, segment 2–3 is not an arc of a circle, due to the action of the stylomandibular ligaments that cause a slight backward movement of the mandible while closing the mouth. Therefore, the position of the condyle in the maximum mouth opening position is more forward than in the maximum protrusion position with the mouth closed. However, in our case, the error, when considering border 2–3 as an arc, is negligible as the MAD allows opening the mouth slightly.

The articular fossa curve is represented in Fig. 4b by straight line Q-Q' with angle α with respect to the occlusal plane. Points Q and Q' are the maximum and minimum values of the original temporomandibular fossa curve. The model considers that the center of the condyle moves through straight line C_{Re}-C_{Pr} parallel to Q-Q' at distance R_c (condyle radius). Again, a scanner or x-ray of the patient's mandible is required to measure the condyle radius and the position of points Q and Q'. Once these values are known, the x-y coordinates of the center of the condyle for the maximum protruded and retruded positions can be obtained.

Angle α between line Q-Q' and the occlusal plane can be calculated with Eq. (2).

$$\alpha = \text{atan} \frac{y_{Q'} - y_Q}{x_{Q'} - x_Q} \tag{2}$$

The straight line that goes through points Q and Q' can be formulated as:

$$y = (x - x_{Q'}) \cdot \tan \alpha + y_{Q'} \tag{3}$$

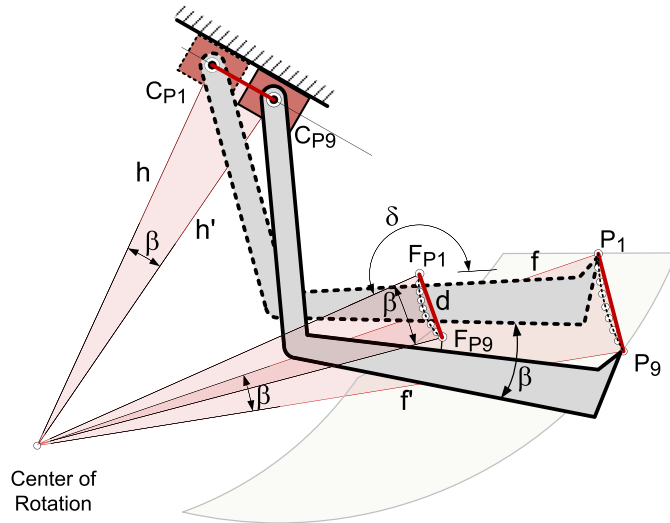


Fig. 5. Center of Rotation of the mandible when the lower incisor moves from P₁ to P₉.

The condyle path can be defined by the equation of a straight line parallel to QQ' at distance R_c:

$$y - y_{Q'} + Rc \cdot \cos \alpha = (x - x_{Q'} - Rc \cdot \sin \alpha) \cdot \tan \alpha \tag{4}$$

The position of point C_{Re} can be obtained by finding the intersection between the condyle path and an arc with radius ML and center A₁. Point C_{Re} coordinates (x_{C_{Re}}, y_{C_{Re}}) can be cleared from Eq. (5).

$$\begin{aligned} y_{C_{Re}} - y_{Q'} + Rc \cdot \cos \alpha &= (x_{C_{Re}} - x_{Q'} - Rc \cdot \sin \alpha) \cdot \tan \alpha \\ (x_{C_{Re}} + Re)^2 + (y_{C_{Re}})^2 &= ML^2 \end{aligned} \tag{5}$$

In the same way, x_{C_{Pr}} and y_{C_{Pr}} can be calculated by finding the intersection between the condyle path and an arc with radius ML and center A₂:

$$\begin{aligned} y_{C_{Pr}} - y_{Q'} + Rc \cdot \cos \alpha &= (x_{C_{Pr}} - x_{Q'} - Rc \cdot \sin \alpha) \cdot \tan \alpha \\ (x_{C_{Pr}} - Pr)^2 + (y_{C_{Pr}})^2 &= ML^2 \end{aligned} \tag{6}$$

Finally, point 3 can be calculated by finding the intersection between an arc with its center in the upper incisor and radius MO and another arc with radius ML and center C_{Pr} (see Fig. 4a). The Cartesian coordinates of point 3 (x₃, y₃) can be cleared from Eq. 7.

$$\begin{aligned} (x_3)^2 + (y_3 - y_g)^2 &= MO^2 \\ (x_3 - x_{C_{Pr}})^2 + (y_3 - y_{C_{Pr}})^2 &= ML^2 \end{aligned} \tag{7}$$

Where y_g is the George gauge bite.

3. Optimal cam design

With the procedure described in the previous section, a methodology is developed to obtain a part of Posselt's diagram, which defines the lower incisor movement limits when opening the mouth. In order to maintain the jaw in a protruded position, a curve to be followed by the lower incisor while opening the mouth, is defined inside the area enclosed by Posselt's diagram. Fig. 5 shows an example of this curve, {P₁,...,P₉} on the dotted line, which allows mouth opening with a forward mandibular motion until the lower incisor reaches point P₉. At this point, the jaw cannot open any further because it has reached its maximum protrusion. The main target is to force the jaw to move forward progressively, so that the more the mouth is opened, the more forward the mandible moves. This requirement affects the curvature of the trajectory that can be used. A wrong curve would make the mandible go backward at a certain stage. The shape of this curve is mainly affected by the initial protrusion and the maximum mouth opening allowed by the oral appliance. Low values of the latter have a negative effect on patient acceptance [48]. On the other side, high values may reduce oropharyngeal airspace [49].

The position of the center of the condyle (x_{C_{Pi}}, y_{C_{Pi}}) for each position of the lower incisor (x_{P_i}, y_{P_i}) is calculated by finding the intersection between the condyle path and an arc with radius ML and its center in the lower incisor position:

$$\begin{aligned} y_{C_{Pi}} - y_{Q'} + Rc \cdot \cos \alpha &= (x_{C_{Pi}} - x_{Q'} - Rc \cdot \sin \alpha) \cdot \tan \alpha \\ (x_{C_{Pi}} + x_{P_i})^2 + (y_{C_{Pi}} + y_{P_i})^2 &= ML^2 \end{aligned} \tag{8}$$

When the lower incisor moves from point P_1 to point P_9 , the center of the condyle moves from point C_{P_1} to point C_{P_9} and the mandible rotates angle β (see Fig. 5). The Center of Rotation (CR) of this movement is situated in the intersection of the perpendicular bisectors to segments $C_{P_1}-C_{P_9}$ and P_1-P_9 . Then, the displacement of the center of the follower, $F_{P_1}-F_{P_9}$, is calculated considering its movement a rotation about the CR along angle β .

Once the path for the lower incisor has been defined, it is discretized with several points on it. In Fig. 5, nine points, $\{P_1, \dots, P_9\}$, are used to discretize the curve on the dotted line. In order to calculate the cam profile, the segments defined by two consecutive points of the positions considered for the lower incisor are used. Each CR is found by defining the length of sides f and h of the triangles shown in Fig. 5. Considering that side f_i has to be equal to f_i' and h_i equal to h_i' , the x-y coordinates of the CR (x_{CR_i} and y_{CR_i}) for displacement P_i-P_{i+1} of the lower incisor is cleared from Eqs. (9) and (10).

$$f_i = \sqrt{(x_{CR_i} - x_{P_i})^2 + (y_{CR_i} - y_{P_i})^2} = \sqrt{(x_{CR_i} - x_{P_{i+1}})^2 + (y_{CR_i} - y_{P_{i+1}})^2} \quad (9)$$

$$h_i = \sqrt{(x_{CR_i} - x_{C_{P_i}})^2 + (y_{CR_i} - y_{C_{P_i}})^2} = \sqrt{(x_{CR_i} - x_{C_{P_{i+1}}})^2 + (y_{CR_i} - y_{C_{P_{i+1}}})^2} \quad (10)$$

The angle of rotation of the mandible, β_i , can be determined with Eq. (11).

$$\beta_i = 2 \cdot \arcsin\left(\frac{\sqrt{(x_{P_i} - x_{P_{i+1}})^2 + (y_{P_i} - y_{P_{i+1}})^2}}{2 \cdot f_i}\right) \quad (11)$$

Finally, in order to know the position of the center of the follower, its displacement d_i from position F_{P_i} to $F_{P_{i+1}}$ and the angle of its radius of rotation (δ_i) are calculated with Eqs. (12) and (13) (see Fig. 5).

$$d_i = 2 \cdot \sqrt{(x_{CR_i} - x_{F_{P_i}})^2 + (y_{CR_i} - y_{F_{P_i}})^2} \cdot \sin\left(\frac{\beta_i}{2}\right) \quad (12)$$

$$\delta_i = \arctan\left(\frac{y_{CR_i} - y_{F_{P_i}}}{x_{CR_i} - x_{F_{P_i}}}\right) \quad (13)$$

The x and y coordinates of the center of the follower in position $i+1$ are obtained with Eqs. (14) and (15), respectively.

$$x_{F_{P_{i+1}}} = x_{F_{P_i}} + d_i \cdot \cos\left(\delta_i + \frac{\Pi}{2} - \frac{\beta_i}{2}\right) \quad (14)$$

$$y_{F_{P_{i+1}}} = y_{F_{P_i}} + d_i \cdot \sin\left(\delta_i + \frac{\Pi}{2} - \frac{\beta_i}{2}\right) \quad (15)$$

With the methodology developed above, the position of the center of the follower is calculated when the lower incisor moves from P_1 to P_9 . In order to obtain the cam profile, a curve that passes through the center of the follower has to be found. To do so, a Bezier curve with four control points is used. This curve is formulated with Eq. (16) where $x_{B_{20}}$, $y_{B_{20}}$ and $x_{B_{23}}$, $y_{B_{23}}$ are the x-y coordinates of the first and last control points respectively. The position of these two control points is known as they coincide with the first and last position of the center of the follower. Parameters t_1 and t_9 , whose values are 0 and 1 respectively, define the first and last position of the center of the follower on the Bezier curve.

$$\begin{aligned} x_{F_{P_i}}(t) &= a_x t^3 + b_x t^2 + c_x t + x_{B_{20}} \\ y_{F_{P_i}}(t) &= a_y t^3 + b_y t^2 + c_y t + y_{B_{20}} \\ c_x &= 3(x_{B_{21}} - x_{B_{20}}) \\ b_x &= 3(x_{B_{22}} - x_{B_{21}}) - c_x \\ a_x &= x_{B_{23}} - x_{B_{20}} - c_x - b_x \\ c_y &= 3(y_{B_{21}} - y_{B_{20}}) \\ b_y &= 3(y_{B_{22}} - y_{B_{21}}) - c_y \\ a_y &= y_{B_{23}} - y_{B_{20}} - c_y - b_y \end{aligned} \quad (16)$$

An optimization process allows finding the unknowns of the Bezier curve with a predefined minimum error. This process is carried out by means of an evolutionary algorithm called MUMSA (Malaga University Mechanism Synthesis Algorithm), developed by the Malaga University research group the authors belong to. Any other optimization method could be used provided it can deal with the constraints the mechanism has. However, evolutionary algorithms are an adequate approach since they provide accurate results in little time with low computational effort. Besides, the algorithm code can easily be modified to adapt to new curves or constraints.

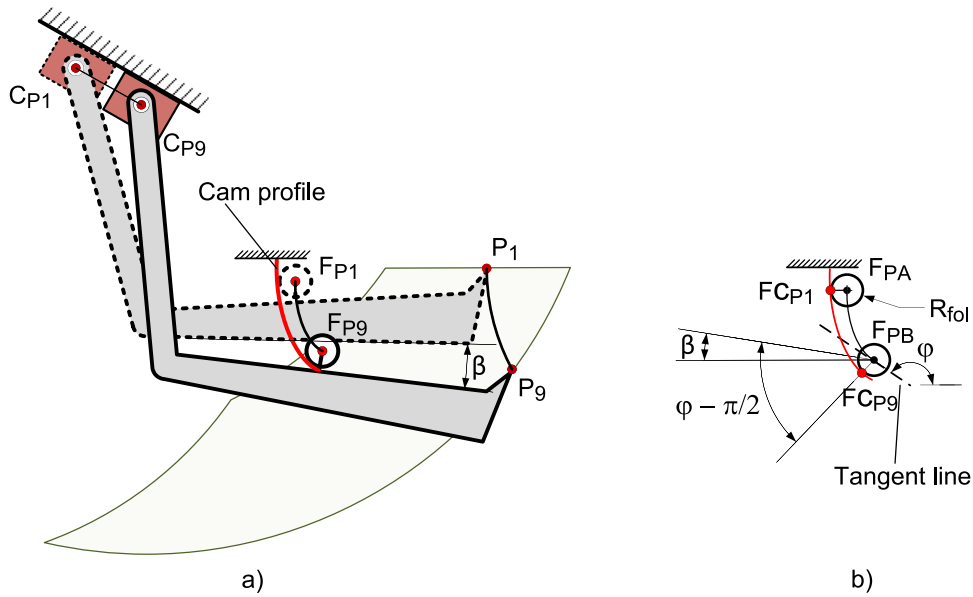


Fig. 6. (a) Profile of a cam linked to the maxilla that forces the mandible to move so that the lower incisor moves from P₁ to P₉. (b) First and last contact point between the cam and the follower.

The algorithm begins by generating a starting population of NP individuals randomly. Each individual is defined by the design variables of the problem whose values are generated randomly within the searching space. For the problem we are dealing with, the design variables are the second and third control points of the Bezier curve ($x_{B_{Z2}}, y_{B_{Z2}}, x_{B_{Z3}}, y_{B_{Z3}}$) and parameter t for points 2 to 8. Value t has to be optimized to know the positions of points 2 to 8 on the Bezier curve in order to evaluate the objective function properly:

$$\begin{aligned} \chi &= [x_{B_{Z1}}, y_{B_{Z1}}, x_{B_{Z2}}, y_{B_{Z2}}, t_2, t_3, t_4, t_5, t_6, t_7, t_8] \in \mathfrak{R} \\ \text{Subject to: } &t_1 = 0, t_9 = 1 \\ &x_{B_{Z0}} = x_{F_{P1}}, y_{B_{Z0}} = y_{F_{P1}} \\ &x_{B_{Z3}} = x_{F_{P9}}, y_{B_{Z3}} = y_{F_{P9}} \end{aligned} \quad (17)$$

To create a new population, reproduction and mutation operators are applied. In the selection process, the best individual and two individuals randomly selected with uniform distribution create disturbing vector V [50]. In this process, a probability factor, F , is used to control the disturbance of the best individual. Next, V is crossed over with individual i of the current population to generate a new individual of the next population. If the latter is better than its antecedent, it will replace it. Crossover is carried out with a probability defined as $CP \in [0, 1]$.

The last procedure is mutation. Depending on the mutation probability, a randomly selected parameter (design variable) can be chosen to mutate by adding $\pm range$ to its original value. Mutation is carried out with a probability defined as $MP \in [0, 1]$.

The algorithm finishes when it reaches the maximum number of iterations or when the error is less than the minimum predefined value.

The optimization problem consists of minimizing the objective function that compares two individuals of a population. Eq. (18) represents the objective function used in this work to find the Bezier curve that reproduces the follower path best. The function calculates the average quadratic error between the points on the follower center path and the points on the Bezier curve:

$$\sum_{i=1}^n \left[(x_{F_{P_i}}(\chi) - x_{F_{P_i}})^2 + (y_{F_{P_i}}(\chi) - y_{F_{P_i}})^2 \right] \quad (18)$$

Where n is the number of positions, χ has been defined in Eq. (17) and $x_{F_{P_i}}$ and $y_{F_{P_i}}$ have been calculated in Eqs. (14) and (15).

Next, the procedure to find the cam profile is developed. The problem can be solved with the follower joined to the mandible and the cam to the maxilla (Fig. 6a) or with the follower joined to the maxilla and the cam to the mandible (Fig. 7). In the first case, the cam is fixed whereas, in the second case, it moves with the mandible. These two cases are studied next.

Fig. 6a shows the cam profile when the follower moves with the mandible. The cam profile can be obtained by calculating the contact points ($F_{C_{P_i}}$) between the cam and the follower (see Fig. 6b). As the follower moves with the mandible, the

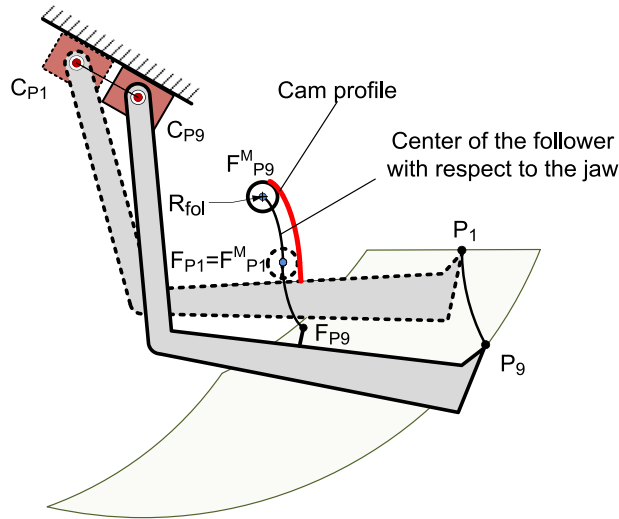


Fig. 7. Path followed by the center of the follower with respect to the mandible. Profile of a cam that moves with the mandible and is pushed by a follower linked to the maxilla.

contact point for the next position of the center of the follower rotates angle β . At the same time, the position of the contact point changes according to the curvature of the cam profile, that is, according to the angle of the line tangent to the path described by the center of the follower (φ).

The position of the contact points are calculated with Eq. (19), where R_{fol} is the radius of the follower:

$$\begin{aligned} x_{F_{C_{pi}}} &= x_{F_{pi}} - R_{fol} \cdot \cos\left(\varphi_i - \frac{\pi}{2} - \beta_i\right) \\ y_{F_{C_{pi}}} &= y_{F_{pi}} - R_{fol} \cdot \sin\left(\varphi_i - \frac{\pi}{2} - \beta_i\right) \end{aligned} \tag{19}$$

Once the contact points are known, the MUMSA algorithm is used to obtain the Bezier curve that defines the cam profile.

In order to obtain the cam profile when the follower is fixed to the maxilla, the relative position of the center of the follower (F_{pi}^M) with respect to the mandible has to be calculated. Points F_{pi}^M are obtained with Eqs. (12)–(15) considering angle β_i to be negative. Fig. 7 shows the path described by the center of the follower with respect to the jaw. The contact points are calculated with Eq. (20).

$$\begin{aligned} x_{F_{C_{pi}}} &= x_{F_{pi}} + R_{fol} \cdot \cos\left(\varphi_i - \frac{\pi}{2} + \beta_i\right) \\ y_{F_{C_{pi}}} &= y_{F_{pi}} + R_{fol} \cdot \sin\left(\varphi_i - \frac{\pi}{2} + \beta_i\right) \end{aligned} \tag{20}$$

Again, the MUMSA algorithm is used to obtain the Bezier curve that goes through the contact points defining the cam profile (see Fig. 7).

4. Real case study

This part applies the methodology, developed in previous sections, to a real case. The cam profile is designed for a follower linked to the maxilla, whose center position ($x_{F_{p1}}$, $y_{F_{p1}}$) is known. A patient’s scanner or X-Ray is used to measure the mandibular length (ML), the condyle radius (R_c) and the x-y coordinates of the maximum (Q) and minimum (Q’) point of the articular fossa curve (see Fig. 8). The rest of the needed values, such as protrusion (Pr), retrusion (Re) and mouth opening (MO), can be measured by an orthodontist or a dentist. All these data are shown in Table 1.

With the measured values, Posselt’s diagram and the desired path for the lower incisor are defined. The latter starts in the initial protrusion position (P_1) and finishes in the maximum mouth opening position (P_9) allowed by the device. Fig. 9a shows borders 1-2-3 of Posselt’s diagram in this case. Line 1-2 is defined with Re and Pr values. Then positions C_{Re} and C_{Pr} of the condyle center are calculated with Eqs. (5) and (6). Finally, border 2-3 is obtained with Eq. (7).

Fig. 9b represents points $\{P_1 \dots P_9\}$ on the desired lower incisor path (see Table 2). The first point, P_1 , on this path is defined with a 40% protrusion and the last one, P_9 , corresponds to 30% MO. The rest of the points are set so that the incisor always moves forward while opening the mouth.

Following the method developed in part 3, the position of the condyle for the nine positions of the lower incisor are calculated with Eq. (8). Next, the centers of rotation for the eight displacements (1 to 9) and angle β , rotated by the mandible in each one of these displacements, are obtained with Eqs. (9)–(11). Finally, the positions of the center of the follower with respect to the mandible are calculated with Eqs. (12)–(15), considering angle β to be negative. These positions are shown in Table 3.

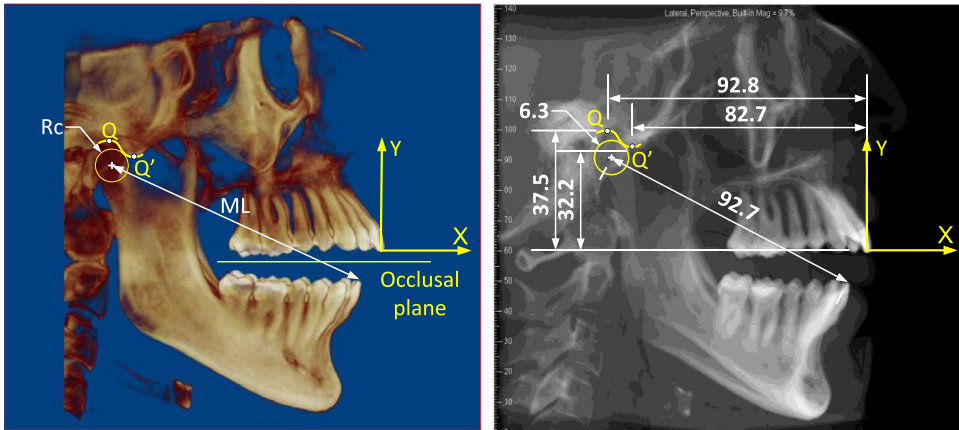


Fig. 8. Scanner and X-Ray of the individual to be studied with measured parameters: mandibular length (ML), condyle radius (Rc) and x- y coordinates of points Q and Q' of the articular fossa curve.

Table 1

Data: follower position (x_{Fp_i} , y_{Fp_i}), mandibular length (ML), condyle radius (Rc), maximum and minimum point of the articular fossa curve (Q, Q'), mouth opening (MO), protrusion (Pr) and retrusion (Re).

x_{Fp_1}	-20 mm
y_{Fp_1}	-3 mm
ML	92.7 mm
Q	[-92.8,37.5] mm
Q'	[-82.7,32.2] mm
Rc	6.3 mm
MO	44 mm
Pr	7 mm
Re	6 mm

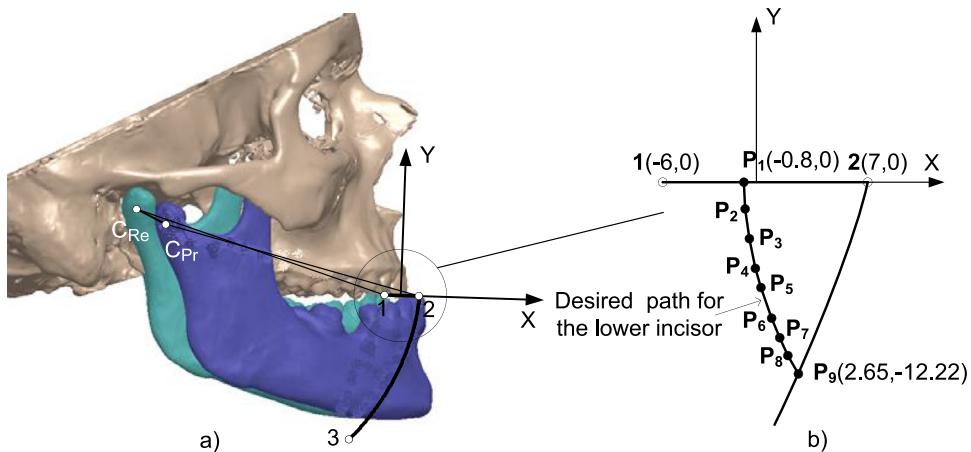


Fig. 9. (a) Scanner of the individual to be studied with the mandible in maximum retrusion and protrusion positions. Posselt's diagram superior border 1-(2) and protruded border 2-(3). (b) Desired path for the lower incisor defined by means of nine points: $\{P_1, \dots, P_9\}$.

The Bezier curve that defines the path of the center of the follower is obtained by means of the optimization process described in Section 3. The following algorithm parameters are used: NP=100, F=0.6, CP=0.4, MP=0.1, range=1 and itermax=1000. The four control points of the curve, t values and the quadratic error, are listed in Table 4.

To know the contact points between the cam and the follower, angles $\{\varphi_1, \dots, \varphi_9\}$ of the tangent lines to the follower path at point P_i have to be previously obtained. To do so, the derivative of the Bezier curve is calculated. Next, the contact points between the follower and the cam are obtained with Eq. (20). The results are shown in Table 5.

Finally, the cam profile is defined by means of a Bezier curve with four control points whose parameters are obtained with the MUMSA algorithm. The optimized values provided by the algorithm are shown in Table 6. This Bezier curve will be

Table 2
Points on the desired path for the lower incisor [mm].

	x_{P_i} [mm]	y_{P_i} [mm]
P ₁	-0.80	0.00
P ₂	-0.71	-1.73
P ₃	-0.46	-3.58
P ₄	-0.05	-5.51
P ₅	0.31	-6.80
P ₆	0.96	-8.71
P ₇	1.47	-9.94
P ₈	2.03	-11.12
P ₉	2.65	-12.22

Table 3
X, Y coordinates of the center of the follower with respect to the mandible.

	$x_{F_i^M}$ [mm]	$y_{F_i^M}$ [mm]
1	-20.00	-3.00
2	-20.07	-1.59
3	-20.34	-0.05
4	-20.83	1.59
5	-21.27	2.61
6	-22.08	4.19
7	-22.72	5.21
8	-23.41	6.17
9	-24.16	7.08

Table 4
Cam Bezier curve of the follower path with respect to the mandible. Known values are shown in **Bold**.

	$B_{Z_i}^X$ [mm]	$B_{Z_i}^Y$ [mm]	t_i [mm]
1	-20.00	-3.00	0.00
2	-19.94	0.37	0.14
3	-21.55	4.09	0.29
4	-24.16	7.08	0.44
5			0.54
6			0.70
7			0.80
8			0.90
9			1.00
Error	$\sum_{i=1}^9 [(x_{R_i}(\chi) - x_{R_i})^2 + (y_{R_i}(\chi) - y_{R_i})^2] = 0.00019 \text{ mm}^2$		

Table 5
Parameters for the cam design: angle of the tangent to the path of the follower center and contact points.

	φ_i°	x_{R_i} [mm]	y_{R_i} [mm]
1	90.85°	-17.00	-3.00
2	97.74°	-17.08	-1.27
3	104.93°	-17.43	0.70
4	111.20°	-18.02	2.67
5	115.28°	-18.55	3.97
6	120.97°	-19.52	5.87
7	124.78°	-20.27	7.08
8	128.53°	-21.09	8.23
9	132.41°	-21.98	9.31

used in a CAD CAM software to shape the cam and assemble it to the dental splint before manufacturing the device with a 3D printer.

5. The device

Once the cam profile has been obtained, a virtual model of the MAD is created. To this purpose, a parametric cam with adjustable geometry depending on the obtained Bezier curve has been previously programmed in a CAD-CAE software. The

Table 6
Bezier curve of the cam profile. Known values are shown in Bold.

	$B_{Z_i}^X$ [mm]	$B_{Z_i}^Y$ [mm]	t_i [mm]
1	-17.00	-3.00	0.00
2	-16.91	1.00	0.14
3	-18.82	5.73	0.30
4	-21.98	9.31	0.45
5			0.55
6			0.70
7			0.80
8			0.90
9			1.00
Error	$\sum_{i=1}^9 [(x_{R_i}(\chi) - x_{R_i})^2 + (y_{R_i}(\chi) - y_{R_i})^2] = 0.00005 \text{ mm}^2$		

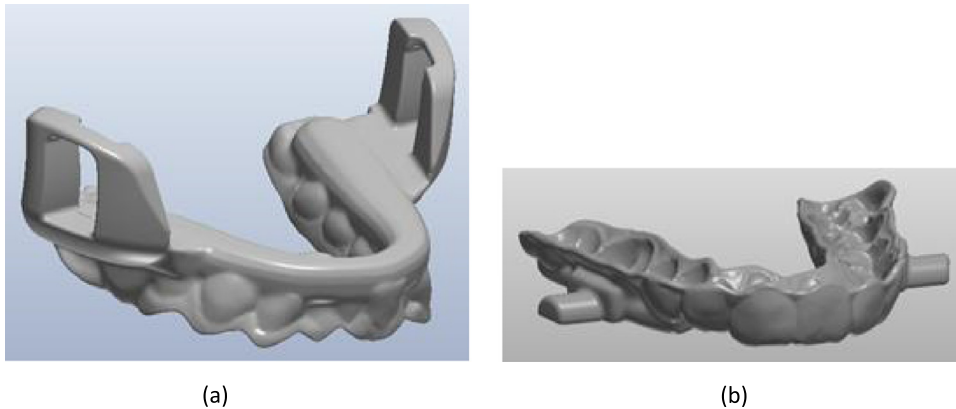


Fig. 10. (a) Mandibular splint with the two cams. (b) Maxilla splint with the two followers.

cam is assembled to a lower dental splint that has previously been modeled using data from a patient's intraoral scanner. Its positioning has to be done precisely considering its angle with the sagittal plane and distance to the lower incisor. The same procedure has to be carried out to assemble the follower to the upper dental splint. In this case, the reference point is the upper incisor.

Fig. 10a shows the lower splint which is joined to the mandible. This splint has two cams, one on each side. Each cam has been reinforced by joining its upper side to a parallel profile, defining a guide the follower moves within.

Fig. 10b displays the upper splint with two cam followers, one on each side. These cam followers have a semicircular profile. They contact the cams with their front side. If the splint separates slightly from the back teeth due to low adherence, the guide touches the back side of the follower, preventing the lower splint from continuing to separate from the teeth. The lateral gap between the upper splint and the cams allows lateral movement.

The model can be sent directly from the CAD-CAE software to a 3D printer to manufacture the device with biocompatible material.

6. Conclusions

In this work a method to design a customized mandibular advancement device has been presented. The device is designed taking into account the kinematic behavior of patients' mandibles thanks to the kinematic analysis of the mandible and the synthesis process followed to generate the cam profile.

The input data can be obtained through an X-ray or a scanner of a patient's jaw and the measurements of protrusion, retrusion and maximum mouth opening taken by a specialist. Once the desired path of the follower has been obtained, the MUMSA algorithm has been used to design the cam that transmits the desired movement to the mandible accurately.

The use of the MUMSA algorithm provides good results in little time with low computational effort, showing its flexibility by adapting it to different kinds of problems.

The definition of the cam profile by means of a curve equation allows its accurate reproduction in a parametric 3D model defined in a CAD-CAE software. Device behavior has been simulated with this model to confirm its correct operation. Finally, the cams are assembled to the patient's dentition model using CAD-CAE software and the device can be manufactured with a 3D printer.

A real case has been included. The proposed methodology has been used to customize a MAD for a patient. The final design has been included in this paper.

Future works will focus on the results obtained in a clinical study with MADs designed following the method described in this paper. Furthermore, asymmetrical temporomandibular joints will also be considered. The use of two cams with different profiles, one for each side, will be needed.

Acknowledgements

A substantial part of the work described in this article was funded by the research contract 806/31.4830 between the private company Laboratorio Ortoplús s.l. and the [University of Malaga](#), which is acknowledged with gratefulness.

References

- [1] J.A. Dempsey, S.C. Veasey, B.J. Morgan, C.P. O'Donnell, Pathophysiology of sleep apnea, *Phys. Rev.* 90 (1) (2010) 47–112, doi:[10.1152/physrev.00043.2008](#).
- [2] A. Malhotra, D.P. White, Obstructive sleep apnoea, *Lancet* 360 (July 20) (2002) 238–245.
- [3] T. Douglas Bradley, J.S. Floras, Obstructive sleep apnoea and its cardiovascular consequences, *Lancet* 373 (January 3) (2009) 82–93 2009.
- [4] H. Wang, J.D. Newton, J.S. Floras, S. Mak, K.-L. Chiu, P. Ruttanaumpawan, G. Tomlinson, T. Douglas Bradley, Influence of obstructive sleep apnea on mortality in patients with heart failure, *J. Am. Coll. Cardiol.* 49 (15) (2007) ISSN 0735-1097/07. Published by Elsevier Inc., doi:[10.1016/j.jacc.2006.12.046](#).
- [5] H. Klar Yaggi, J. Concato, W.N. Kernan, J.H. Lichtman, L.M. Brass, V. Mohsenin, Obstructive sleep apnea as a risk factor for stroke and death, *N. Engl. J. Med.* 353 (November 10) (2005) 2034–2041.
- [6] L.J. Epstein, D. Kristo, J. Strollo Jr, N. Friedman, A. Malhotra, S.P. Patil, K. Ramar, R. Rogers, R.J. Schwab, E.M. Weaver, M.D. Weinstein, Clinical guideline for the evaluation, management and long-term care of obstructive sleep apnea in adults, *J. Clin. Sleep Med.* 5 (3) (2009).
- [7] K. Sutherland, P.A. Cistulli, Mandibular advancement splints for the treatment of sleep apnea syndrome, *Swiss Med. Weekly* 141 (September) (2011) w13276, doi:[10.4414/smww.2011.13276](#).
- [8] K. Sutherland, O.M. Vanderveken, H. Tsuda, M. Marklund, F. Gagnadoux, C.A. Kushida, P.A. Cistulli, Oral appliance treatment for obstructive sleep apnea: an update, *J. Clin. Sleep Med.* 10 (2) (2014) 215–227.
- [9] M. Barnes, R. Douglas McEvoy, S. Banks, N. Tarquinio, C.G. Murray, N. Vowles, R.J. Pierce, Efficacy of positive airway pressure and oral appliance in mild to moderate obstructive sleep apnea, *Am. J. Respir. Crit. Care Med.* 170 (2004) 656–664, doi:[10.1164/rccm.200311-1571OC](#).
- [10] C.L. Phillips, R.R. Grunstein, M. Ali Darendeliler, A.S. Mihailidou, V.K. Srinivasan, B.J. Yee, G.B. Marks, P.A. Cistulli, Health outcomes of continuous positive airway pressure versus oral appliance treatment for obstructive sleep apnea, *Am. J. Respir. Crit. Care Med.* 187 (Apr 15 (8)) (2013) 879–887, doi:[10.1164/rccm.201212-2223OC](#).
- [11] M. Glos, T. Penzel, C. Schoebel, G.-R. Nitzsche, S. Zimmermann, C. Rudolph, A. Blau, G. Baumann, P.-G. Jost-Brinkmann, S. Rautengarten, J.C. Meier, I. Peroz, I. Fietze, Comparison of effects of OSA treatment by MAD and by CPAP on cardiac autonomic function during daytime, *Sleep Breath* 20 (2016) 635–646, doi:[10.1007/s11325-015-1265-0](#).
- [12] D.J. Gale, R.H. Sawyer, A. Woodcock, P. Stone, R. Thomson, K. O'Brien, Do oral appliances enlarge the airway in patients with obstructive sleep apnoea? A prospective computerized tomographic study, *Eur. J. Orthod.* 22 (2000) 159–168.
- [13] E. Sari and S. Menillo. Comparison of titratable oral appliance and mandibular advancement splint in the treatment of patients with obstructive sleep apnea. *Int. Scholarly Res. Network*. Volume 2011, Article ID 581692, 7 pages. doi:[10.5402/2011/581692](#).
- [14] J. Martínez-Gomis, E. Willaert, L. Nogues, M. Pascual, M. Somoza, C. Monasterio, Five years of sleep apnea treatment with a mandibular advancement device, *Angle Orthod.* 80 (1) (2010), doi:[10.2139/030309-122.1](#).
- [15] K.E. Bloch, A. Iseli, J.N. Zhang, X. Xie, V. Kaplan, P.W. Stoelckli, E.W. Russi, A randomized, controlled crossover trial of two oral appliances for sleep apnea treatment, *Am. J. Respir. Crit. Care Med.* 162 (2000) 246–251.
- [16] O.M. Vanderveken, A. Devolder, M. Marklund, A.N. Boudewyns, M.J. Braem, W. Okkerse, J.A. Verbraecken, K.A. Franklin, W.A. De Backer, P.H. Van de Heyning, Comparison of a custom-made and a thermoplastic oral appliance for the treatment of mild sleep apnea, *Am. J. Respir. Crit. Care Med.* 178 (2008) 197–202, doi:[10.1164/rccm.200701-114OC](#).
- [17] M. Deltjens, O.M. Vanderveken, P.H. Van de Heyning, M.J. Braem, Current opinions and clinical practice in the titration of oral appliances in the treatment of sleep-disordered breathing, *Sleep Med. Rev.* 16 (2012) 177–185, doi:[10.1016/j.smrv.2011.06.002](#).
- [18] H.M. Lawton, J.M. Battagel, B. Kotecha, A comparison of the Twin Block and Herbst mandibular advancement splints in the treatment of patients with obstructive sleep apnoea: a prospective study, *Eur. J. Orthod.* 27 (1) (2005) 82–90, doi:[10.1093/ejo/cjh067](#).
- [19] E. Rose, R. Staats, C. Virchow, I.E. Jonas, A comparative study of two mandibular advancement appliances for the treatment of obstructive sleep apnoea, *Eur. J. Orthod.* 24 (2002) 191–198.
- [20] A. Shadaba, J.M. Battagel, A. Owa, C.B. Croft, B.T. Kotecha, Evaluation of the Herbst Mandibular Advancement Splint in the management of patients with sleep-related breathing disorders, *Clin. Otolaryngol.* 25 (2000) 404–412.
- [21] M. Yow, An overview of oral appliances and managing the airway in obstructive sleep apnea, *Semin. Orthod.* 15 (June (2)) (2009) 88–93, doi:[10.1053/j.sodo.2009.01.006](#).
- [22] A.O. de Brito Teixeira, L.B.P. Abi-Ramia, M.A. de Oliveira Almeida, Treatment of obstructive sleep apnea with oral appliances, *Prog. Orthod.* 14 (10) (2013), doi:[10.1186/2196-1042-14-10](#).
- [23] Y.W. Chan, S.K. Sim, Optimum cam design using the Monte Carlo optimization technique, *J. Eng. Des.* 9 (1) (1998) 29–45, doi:[10.1080/095448298261651](#).
- [24] S. Cardona, E.E. Zayas, L. Jordi, P. Català, Synthesis of displacement functions by Bézier curves in constant-breadth cams with parallel flat-faced double translating and oscillating followers, *Mech. Mach. Theory* 62 (2013) 51–62.
- [25] J. Lampinen, Cam shape optimisation by genetic algorithm, *Comput. Aided Des.* 35 (2003) 727–737, doi:[10.1016/S0010-4485\(03\)00004-6](#).
- [26] R.H. Bravo, F.W. Flocker, Optimizing cam profiles using the particle swarm technique, *J. Mech. Des.* 133 (Sep 07 (9)) (2011) 091003 11 pages, doi:[10.1115/1.4004587](#).
- [27] H. Qiu, C.-J. Lin, Z.-Y. Li, H. Ozaki, J. Wang, Y. Yue, A universal optimal approach to cam curve design and its applications, *Mech. Mach. Theory* 40 (2005) 669–692.
- [28] H. Xiao, J.W. Zu, Cam profile optimization for a new cam drive, *J. Mech. Sci. Technol.* 23 (2009) 2592–2602, doi:[10.1007/s12206-009-0715-7](#).
- [29] J. Angeles, C. Lopez-Cajún, Optimal synthesis of cam mechanisms with oscillating flat-face followers, *Mech. Mach. Theory* 23 (1) (1988) 1–6.
- [30] M. Hidalgo-Martínez, E. Sanmiguel-Rojas, M.A. Burgos, Design of cams with negative radius follower using Bézier curves, *Mech. Mach. Theory* 82 (2014) 87–96.
- [31] H. Xiao and J.W. Zu. Evolutionary multi-objective optimisation of cam profile for a new cam drive engine. *Int. J. Veh. Des.*, Volume 53, Issue 3. doi:[10.1504/IJVD.2010.03383](#).
- [32] M. Mandal, T.K. Naskar, Introduction of control points in splines for synthesis of optimized cam motion program, *Mech. Mach. Theory* 44 (2009) 255–271.
- [33] V.-T. Nguyen, D.-J. Kim, Flexible cam profile synthesis method using smoothing spline curves, *Mech. Mach. Theory* 42 (2007) 825–838.
- [34] T. Ouyang, P. Wang, H. Huang, N. Zhang, N. Chen, Mathematical modeling and optimization of cam mechanism in delivery system of an offset press, *Mech. Mach. Theory* 110 (2017) 100–114.
- [35] T. Ouyang, P. Wang, H. Huang, Cam profile optimization for the delivery system of an offset press, *Proc. Inst. Mech. Eng. Part C J. Mech. Eng. Sci.* 231 (23) (2017) 4287–4297.

- [36] L.K. Sahu, V.K. Kedia, M. Sahu, Design of Cam and Follower system using basic and synthetic curves: a review, *Int. J. Innovative Sci., Eng. Technol.* 3 (February (2)) (2016) 362–372.
- [37] J.A. Cabrera, A. Ortiz, F. Nadal, J.J. Castillo, An evolutionary algorithm for path synthesis of mechanisms, *Mech. Mach. Theory* 46 (2011) 127–141.
- [38] J.H. Koolstra, Dynamics of the human masticatory system, *Crit. Rev. Oral Biol. Med.* 13 (4) (2002) 366–376, doi:10.1177/154411130201300406.
- [39] P.U. Dijkstra, A.L. Hof, B. Stegenga, L.G.M. De Bont, Influence of mandibular length on mouth opening, *J. Oral Rehabil.* 26 (1999) 117–122.
- [40] P.U. Dijkstra, L.G.M. De Bont, B. Stegenga, G. Boering, Temporomandibular joint mobility assessment: a comparison between four methods, *J. Oral Rehabil.* 22 (1995) 439–444.
- [41] K.H. Traversa, P.H. Buschanga, H. Hayasakib, G.S. Throckmorton, Associations between incisor and mandibular condylar movements during maximum mouth opening in humans, *Arch. Oral. Biol.* 45 (2000) 267–275.
- [42] L. Merlini, S. Palla, The relationship between condylar rotation and anterior translation in healthy and clicking temporomandibular joints, *Schweiz Monatsschr Zahnmed* 98 (November) (1988) 1191–1199.
- [43] M. Naeije, Local kinematic and anthropometric factors related to the maximum mouth opening in healthy individuals, *J. Oral Rehabil.* 29 (2002) 534–539.
- [44] T. Fukui, M. Tsuruta, K. Murata, Y. Wakimoto, H. Tokiwa, Y. Kuwahara, Correlation between facial morphology, mouth opening ability, and condylar movement during opening-closing jaw movements in female adults with normal occlusion, *Eur. J. Orthod.* 24 (2002) 327–336.
- [45] H.-J. Yoon, K.D. Zhao, J. Rebellatod, K.-N. Anc, E.E. Kellera, Kinematic study of the mandible using an electromagnetic tracking device and custom dental appliance: introducing a new technique, *J. Biomech.* 39 (2006) 2325–2330, doi:10.1016/j.jbiomech.2005.07.001.
- [46] H. Wen, W. Xu, M. Cong, Kinematic model and analysis of an actuation redundant parallel robot with higher kinematic pairs for jaw movement, *IEEE Trans. Indust. Electron.* 62 (3) (march 2015) 1590–1598.
- [47] U. Posset, Studies in the mobility of the human mandible, *Acta Odontol. Scand. Suppl.* 10 (Suppl. 10) (1952).
- [48] A.J. Pitsis, M. Ali Darendeliler, H. Gotsopoulos, P. Petocz, P.A. Cistulli, Effect of vertical dimension on efficacy of oral appliance therapy in obstructive sleep apnea, *Am. J. Respir. Crit. Care Med.* 166 (2002) 860–864, doi:10.1164/rccm.200204-342OC.
- [49] P.R.I. L'Estrange, J.M. Battagel, B. Harkness, M.H. Spratley, P.J. Nolan, G.I. Jorgensen, A method of studying adaptive changes of the oropharynx to variation in mandibular position in patients with obstructive sleep apnoea, *J. Oral Rehabil.* 23 (10) (1996 Oct) 699–711.
- [50] R. Storn, K. Price, Differential evolution. A simple and efficient heuristic scheme for global optimization over continuous spaces, *J. Global Optim.* 11 (1997) 341–359.